DENSITY-BASED METHOD FOR BUILDING DETECTION FROM LiDAR POINT CLOUD

A. Mahphood [1, 2], H. Arefi [1, 3] *

[1] School of Surveying and Geospatial Engineering, College of Engineering, University of Tehran, Tehran, Iran - (ahmadmahphood, hossein.arefi)@ut.ac.ir
[2] Faculty of Surveying and Geomatic Engineering, Tishreen University, Latakia, Syria - ahmadmahphood@tishreen.edu.sy
[3] i3mainz – Institute for Spatial Information and Surveying Technology, Mainz University of Applied Sciences, Germany - hossein.arefi@hs-mainz.de

Commission IV, WG IV/3

KEY WORDS: LiDAR Point Cloud, Building Detection, Density, Vegetation Removal, Tornado, Cube.

ABSTRACT:

In this paper, a new building detection method based on a density of LIDAR point clouds is proposed. In this method, trees, vegetation, and any objects that have points in a vertical plane or column are removed. In the density-based method, a cube is utilized to calculate the density therein. For each point, the cube is used to determine the number of neighbouring points. The density is calculated in two cases: 3D and 2D space. In 3D space, the volumetric density is calculated using the cube. In 2D space, all points are projected onto the horizontal plane, and the surface density is calculated using a square. Next, the two densities are compared and the points with different values in both cases are removed. The method leads to promising results in the removal of vegetation and trees. Moreover, the results achieve more than 94% completeness and correctness at the per-area level.

1. INTRODUCTION

Airborne LiDAR (Light Detection And Ranging) and photogrammetry point clouds are nowadays employed to produce high-quality features and models. These datasets are very efficient data for different applications in photogrammetry and remote sensing, such as building detection (Yi et al., 2021), 3D building reconstruction (Mahphood and Arefi, 2017, Tarsha Kurdi et al., 2021, Yastikli and Cetin, 2021), digital terrain model (DTM) generation (Mongus and Žalik, 2012), change detection (Liu et al., 2021), ground point filtering (Zeybek and Şanlıoğlu, 2019), point cloud registration (Favre et al., 2021), as well as building boundary extraction (Widyaningrum et al., 2019, Mahphood and Arefi, 2022).

One of the most important research fields in remote sensing and photogrammetry is building detection. In general, detecting the building from the LiDAR data depends on the removing of the other objects (Sajadian and Arefi, 2014, Awrangjeb and Siddiqui, 2017, Mahphood and Arefi, 2020b). The main objects that pose the greatest challenge to building detection are vegetation and ground. These objects have the greatest size in the dataset. For the removal of ground points, some studies have used DTM for this purpose (Dorninger and Pfeifer, 2008, Awrangjeb and Fraser, 2014, Awrangjeb et al., 2014, Awrangjeb and Siddiqui, 2017). Another study used a threshold as a flat plane. It is used if the region is flat (Sajadian and Arefi, 2014). However, for mountainous areas, the previous method cannot be carried out. Other studies have used commercial software (Ao et al., 2017). Some methods use the morphological method, which is not affected by the area type (Arefi and Hahn, 2005, Cheng et al., 2013). Neidhart and Sester (2008) used a mathematical model (polynomial). Mahphood and Arefi (2020b) detected the buildings without handling the ground point filtering issue using the virtual first and last pulse method. For vegetation removal, most of the methods use features that are extracted using textural and spatial information to remove the vegetation points. These features are flatness, distribution of neighbourhood points, curvature, eigenvalue features, a variance of normal directions, etc. (Alharthy and Bethel, 2002, Forlani et al., 2006, Ekhtari et al., 2008, Maltezos and Ioannidis, 2015, Hui et al., 2016, Mahphood and Arefi, 2020b). The information of pulses has been used to remove the vegetation from LiDAR data (Alharthy and Bethel, 2002, Vögtle and Steinle, 2005, Tarsha-Kurdi et al., 2007, Niemeyer et al., 2011, Shiravi et al., 2012, Hui et al., 2016, Mahphood and Arefi, 2020b).

This paper proposed a novel method to detect the buildings from the LiDAR point cloud by removing the vegetation, trees, and objects that have points located in the imaginary column. The proposed method used a volumetric shape (cubic) to detect the density for each point in two cases: 3D and 2D space. Depending on the density difference between the two cases, the points are removed or retained.

2. THE PROPOSED METHOD

Figure 1 explains the workflow of the proposed method. At first, the noise points are removed. Then, the ground points are filtered by the tornado method. After that, the vegetation and trees are removed by the density method. Finally, the resulting buildings are refined using some other filters.

2.1 Pre-processing

The noise points should be removed because they significantly affect the results of the proposed method, which depends on the points located in the imaginary column; therefore, the accuracy will be affected if the noise points are used in the other processing

* Corresponding author

steps. The CloudCompare software is utilized to implement this step. It utilizes the statistical outlier removal method, which averages the distances between adjacent points to remove the noise points.

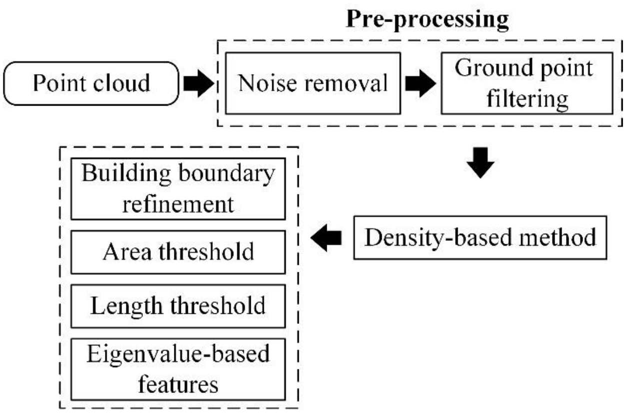

Figure 1. Workflow of the proposed method.

Ground point filtering is considered one of the most important challenges in building detection because the ground points have the most significant number of points. This paper uses the tornado method for this purpose (Mahphood and Arefi, 2020a). This method simulates a realistic tornado for removing objects from the ground. A vertical cone models the tornado so its vertex is down and its base is up (Figure 2(a)). The cone moves on the ground surface using a series of points selected as vertices. Points that are inside the cone are classified as non-ground points and removed (Figure 2(b)).

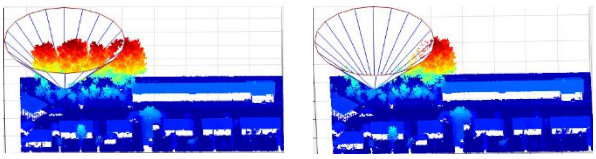

(a) (b)

Figure 2. Tornado method. a) The vertical cone, and b) the procedure of point removal. In (Mahphood and Arefi, 2020a)

2.2 Density-Based Method

After the previous step, the remaining objects are trees, vegetation, and small objects. For filtering these objects, the density of points in 3D and 2D space is used. First, the neighborhood density of each point is calculated using a cube (with dimensions: length l, width w, and height h as shown in Figure 3(a)) in the three-dimensional space (volumetric density). Then, these points are projected on a horizontal x-y plane, and the density of the points is calculated using the cube (surface density as shown in Figure 3(b)). Then, the points of the walls, power lines, trees, and vegetation are removed by comparing the two densities. In other words, all objects with points in the vertical plane or vertical column will be removed. Thus, the remaining points are related to the building and some small objects, which will be handled in the next step.

After obtaining the preliminary detected buildings, several sparse points have not been removed. Furthermore, the building outlines are affected due to the findings of the density method in the vegetation removal step. As a result, three filters are used to improve the results.

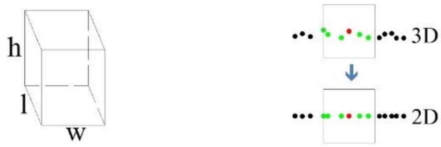

(a) (b)

Figure 3. Density-based method. a) The used cube dimensions to detect the neighborhood of each point, b) detecting the point neighborhood in 3D and 2D space. The red and green points represent the interest points and the points inside the cube, respectively.

2.2.1 Building Boundary Refinement: The points of the building boundaries are removed because of using the cubic for vegetation removal. Thus, the detected buildings should be refined. Therefore, the nearest neighbor method adds points from the removed points. Where the used threshold of the nearest neighbor is equal to half the cube width.

2.2.2 Area Threshold: A few tiny regions are leftover from plants or objects that aren't recognized as buildings. As a result, an area threshold T_a is utilized to eliminate these regions.

2.2.3 Length Threshold: Because of the use of the tornado method to filter the ground points, ground regions related to longitudinal objects, such as rivers, are not filtered well. As a result, a length threshold T_l is used to remove these regions.

2.2.4 Eigenvalue-Based Feature: Some trees and vegetation are impenetrable. Therefore, their points cannot be removed using the density method. To handle this issue, the eigenvalue-based feature is utilized. Where the eigenvalues ($\lambda 1$, $\lambda 2$ and $\lambda 3$) are extracted. The feature $\lambda 3$ is used for this step (Ao et al., 2017, Mahphood and Arefi, 2020b).

3. EXPERIMENTAL RESULTS AND ANALYSIS

3.1 Data Description

To evaluate the results, the LiDAR point cloud of the 2015 IEEE GRSS dataset is used (Figure 4). The dataset contains an urban and harbour area in Zeebruges, Belgium. The point cloud density is 65 points/m². In other words, the point spacing is about 10 cm.

Figure 4. IEEE dataset.

3.2 Evaluation System

The qualitative and quantitative assessments are described in this section. For the qualitative assessment, the detected buildings and other detected objects will be discussed visually. For the quantitative assessment, the metrics of CP completeness (%), CR correctness (%), and Q quality (%) (equations (1)-(3)) are computed for the results on a per-object and per-area level (Rutzinger et al., 2009). Unfortunately, there is no reference data for the dataset. Thus, reference data is extracted manually using an orthophoto for the same areas.

$$CP = \frac{\mathrm{TP}}{\mathrm{TP+FP}} \tag{1}$$

$$\mathrm{CR} = \frac{\mathrm{TP}}{\mathrm{TP + FN}} \tag{2}$$

$$Q = \frac{\mathrm{TP}}{\mathrm{TP + FP + FN}} \tag{3}$$

where TP, FP, and FN indicate a true positive, a false positive, and a false negative, respectively.

3.3 Density-Based Method Evaluation

3.3.1 Horizontal Dimensions Analysis of the Cube (length *l* and width *w*): To analyze the horizontal dimensions of a cube, we see from Figure 5(a) that the minimum width and length must be greater than the point cloud density. Because if the dimensions are less than the density, the density inside the cube is not found at any point (red point), and the method becomes meaningless (Figure 5 (b)). Also, in this cube, the length is always equal to the width.

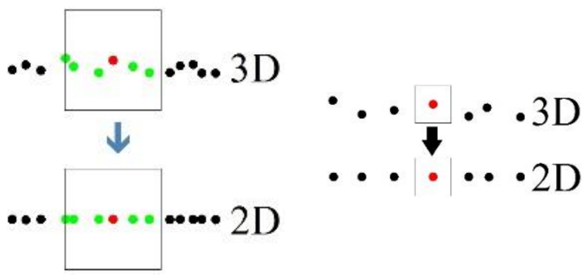

(a) (b)

Figure 5. The cube dimensions are greater than density (a) or less than density (b). The green points are the points inside the cube. The black points are the points outside the cube.

The main purpose of the density-based method is to remove vegetation and tree points. Therefore, the effect of the horizontal dimensions of the cube on the count of the removed points should be investigated. To evaluate these parameters and select the best values, nine sets of tree points are extracted manually from the data (Tr1, Tr2, Tr3, Tr4, Tr5, Tr6, Tr7, Tr8, and Tr9). After that, the density-based method is used for different width values (or length), and the removed points percentage is computed for each value and each set. The method is implemented for nine width values, so we start with a width equal to the mean density *D*. It is increased by the amount of density until we reach ten times the density.

Obviously, if the width increases, the removal percentage will increase (Table 1). The lowest width should be selected so that this width has a high removal ratio. The width should also be small because the greater width will affect the height (this effect is analyzed in the next step). Also, the removal percentage is higher for greater width. Therefore, the width at which the percentage is at least 99% is selected to ensure the best results. From Figure 6, it can be seen that widths equal to 2.5D and more are the best widths that guarantee the previous percentage. Thus, a distance of 3D is utilized to ensure the best results. The results of mean values of the groups' results are shown in Table 1 and Figure 6(b). These results prove that this method has promising results for removing vegetation points from the LiDAR data. At the same time, this process is an essential step for detecting buildings.

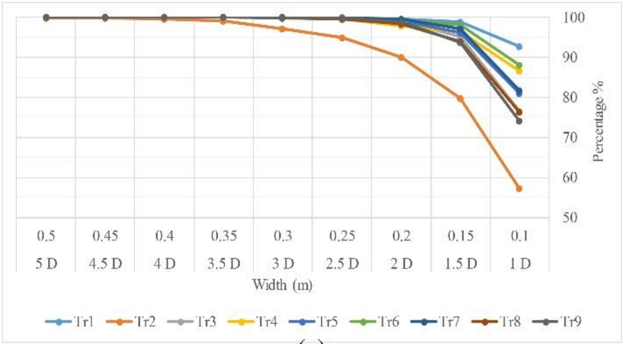

(a)

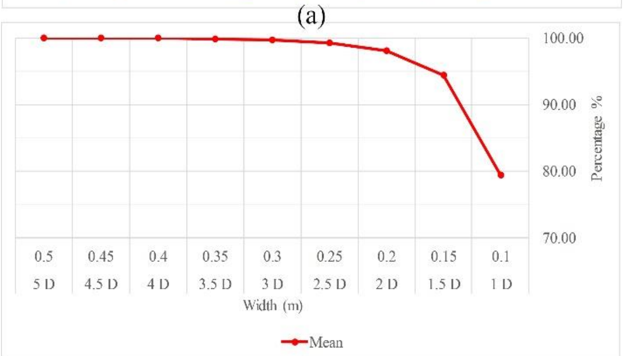

(b)

Figure 6. The relationship between the cube width and the removal percentage. a) Results of nine tree sets, b) Average results.

1 *D*	1.5 *D*	2 *D*	2.5 *D*	3 *D*	3.5 *D*	4 *D*	4.5 *D*	5 *D*
79.39	94.36	98.04	**99.21**	**99.63**	**99.89**	**99.96**	**99.98**	**99.98**

Table 1. Average results for nine tree sets. (The best values are bold, and *D* refers to the average density).

3.3.2 Cube Height Analysis: This method may remove roof points for the high-slope building roofs (Figure 7). From Figure 7(a), we see roof points inside the cube in the 2D space. But they are outside the cube in the 3D space (blue points). Therefore, the roof points will be removed. To handle this issue, the relationship between the cube height, cube width, and the largest inclination angle θ of the roof is found. From Figure 7(b), the relationship between the previous parameters can be expressed by equation (4) so that the roof points are not removed. The angle θ is assumed according to the knowledge of the roof slope of the existing buildings where it cannot be calculated accurately.

$$h_{min} >= w \times \tan\theta \tag{4}$$

where θ = largest inclination angle of the roofs.
h_{min} = the minimum height of cube.
W = cube width.

https://doi.org/10.5194/isprs-annals-X-4-W1-2022-423-2023 | © Author(s) 2023. CC BY 4.0 License.

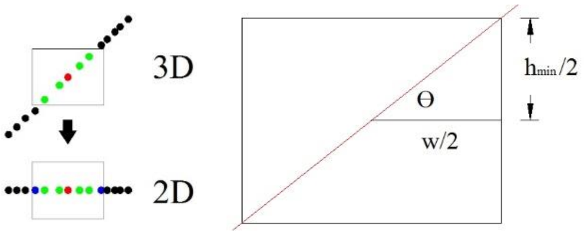

(a) (b)

Figure 7. Issue of the building roof with a steep slope. a) The difference between the number of neighborhood points in the 3D and 2D space, b) The relationship between the minimum height, width, and the inclination angle of the roof. The red line is the building roof. The red, green, and blue points represent the interest, the neighborhood, and the new points in 2D space, respectively.

3.4 Building Detection Evaluation

3.4.1 Overall Results and Evaluation: The results of the proposed method for detecting the building are shown in Figure 8, with some advantages and disadvantages.

For qualitative assessment, it can be seen from Figure 8 that small, large, residential, and complex buildings (Figure 8(f)) are successfully detected. According to Figure 8(f), the method detects the buildings that contain sloping, flat, and hipped roofs. Also, the buildings which have one or a block of buildings are detected (Figure 8(f)). This is an advantage of our method. Also, we see that all trees and vegetation are removed successfully using the density-based method. As an initial vision, the results are excellent, especially with regard to removing vegetation points and detecting different shapes of buildings. Our method achieves promising results. However, some problems arose during the procedure.

Some buildings (Figure 8(e)) are not fully detected because trees surround some parts of the building. These parts are occluded areas that are not detected by this method. Also, we note from Figure 8(f) that the building boundaries (inner and outer) that have height displacement were removed. This is because the points of the outer and inner walls and the neighbouring points were removed. Where the density of each point was different between 3D and 2D space. For vegetation, some vegetative walls are not removed, as shown in Figure 8(c). They have a flat surface and are non-penetrated. The cars are removed. But some are not removed (Figure 8(d)). Because they are behind each other and considered as a large object. Figure 8(b) shows that some ground points are not filtered. This problem is due to the ground filtering step. The cone (tornado) did not remove the river points completely. This is because these points have a high slope.

For quantitative assessment, the metrics: completeness, correctness, and quality are computed and listed in Table 2 for the IEEE 2015 data. From Table 2, our method obtains 94.17% completeness, 94.66% correctness, and 89.44% quality at the per-area level and 91.53% completeness, 82.63% correctness, and 76.75% quality at the per-object level. Also, it obtains the completeness of 100%, correctness, and quality of 96.4% for the buildings whose areas are larger than 50 m^2. As a result, the density-based method provides promising results, especially at the per-area level, where the completeness and correctness are more than 94%. Also, these results provide promising results for completeness metrics for all levels. Also, these results are very good for buildings whose areas are larger than 50 m^2. Correctness is relatively low due to the presence of unfiltered ground points.

(a)

(b) (c) (d)

(e) (f)

Figure 8. The results of the building detection. a) Results: false-negative FN (blue), true positive TP (yellow), and false-positive FP (red), (b)-(f) Examples of TP, FP, and FN.

Metric	Per-area (%)	Per-object (%)	Per-object > 50 m^2 (%)
CP	94.17	91.53	100
CR	94.66	82.63	96.4
Q	89.44	76.75	96.4

Table 2. The results of the building detection.

3.4.2 Parameters Analysis: There are two important parameters that affect the results. The first one is the cube width. This parameter was analyzed previously. The second one is the slope angle of the building roof to calculate the cube height. This angle is set to 70 degrees. The area threshold T_a is set to 9 m^2, as most buildings in the IEEE 2015 data are interconnected and large. For the length threshold, T_l is set to 200 m, as most buildings are less than 100 m. The eigenvalue λ_3 shows the spatial difference in the vertical direction. Thus, $\sqrt{\lambda_3}$ is used as the standard deviation and set to 5 cm.

4. CONCLUSION

A novel method has been proposed for tress and vegetation removal by using the density inside a cube in 2D and 3D space to detect the buildings from the LiDAR point cloud. The density-based method used a cube with dimensions related to the point cloud density and the maximum roof slope. The results achieve the completeness of 94.17%, correctness of 94.66%, and quality of 89.44% for the per-area level. Also, the method provides promising results for completeness metrics for all levels. The small, large, and complex buildings are detected well. In other words, the type or size of roofs does not affect the results of the proposed method. Also, the trees and vegetation are removed perfectly. This is an essential step for the methods of building detection.

Finally, our method is very good for detecting buildings with different shapes, sizes, and heights. But the building boundaries are affected slightly. Also, the method cannot extract the occluded areas of the buildings surrounded by trees. This issue is considered the major disadvantage of our method.

REFERENCES

Alharthy, A. and J. Bethel, 2002. Heuristic filtering and 3D feature extraction from LIDAR data. *Int. Arch. Photogramm. Remote Sens. Spatial Inf. Sci.* 34(3/A): 29-34.

Ao, Z., Y. Su, W. Li, Q. Guo and J. Zhang, 2017. One-Class Classification of Airborne LiDAR Data in Urban Areas Using a Presence and Background Learning Algorithm. *Remote Sensing* 9(10): 1001. DOI: 10.3390/rs9101001.

Arefi, H. and M. Hahn, 2005. A morphological reconstruction algorithm for separating off-terrain points from terrain points in laser scanning data. *Int. Arch. Photogramm. Remote Sens. Spatial Inf. Sci.* 36(3/W19): 120-125.

Awrangjeb, M. and C. Fraser, 2014. Automatic segmentation of raw LiDAR data for extraction of building roofs. *Remote Sensing* 6(5): 3716-3751. DOI: 10.3390/rs6053716.

Awrangjeb, M., G. Lu and C. Fraser, 2014. Automatic building extraction from LiDAR data covering complex urban scenes. *Int. Arch. Photogramm. Remote Sens. Spatial Inf. Sci.* 40(3): 25.

Awrangjeb, M. and F. U. Siddiqui, 2017. a New Mask for Automatic Building Detection from High Density Point Cloud Data and Multispectral Imagery. *ISPRS Ann. Photogramm. Remote Sens. Spatial Inf. Sci.* 4: 89. DOI: 10.5194/isprs-annals-IV-4-W4-89-2017.

Cheng, L., W. Zhao, P. Han, W. Zhang, J. Shan, Y. Liu and M. Li, 2013. Building region derivation from LiDAR data using a reversed iterative mathematic morphological algorithm. *Optics Communications* 286: 244-250. DOI: 10.1016/j.optcom.2012.08.028.

Dorninger, P. and N. Pfeifer, 2008. A comprehensive automated 3D approach for building extraction, reconstruction, and regularization from airborne laser scanning point clouds. *Sensors* 8(11): 7323-7343. DOI: 10.3390/s8117323.

Ekhtari, N., M. Sahebi, M. V. Zoej and A. Mohammadzadeh, 2008. Automatic building detection from LIDAR point cloud data. *21st ISPRS Congress, Commission, WG IV/3, Beijing, China*.

Favre, K., M. Pressigout, E. Marchand and L. Morin, 2021. A plane-based approach for indoor point clouds registration. *2020 25th International Conference on Pattern Recognition (ICPR)*: 7072-7079. DOI: https://doi.org/10.1109/ICPR48806.2021.9412379.

Forlani, G., C. Nardinocchi, M. Scaioni and P. Zingaretti, 2006. Complete classification of raw LIDAR data and 3D reconstruction of buildings. *Pattern Analysis and Applications* 8(4): 357-374. DOI: 10.1007/s10044-005-0018-2.

Hui, Z., Y. Hu and Y. Yevenyo, 2016. AUTOMATIC BUILDING EXTRACTION FROM AIRBORNE LIDAR POINT CLOUD BASED ON MEAN SHIFT SEGMENTATION. *GEOBIA 2016 : Solutions and Synergies., 14 September 2016 - 16 September 2016, University of Twente Faculty of Geo-Information and Earth Observation (ITC)*.

Liu, D., D. Li, M. Wang and Z. Wang, 2021. 3D Change Detection Using Adaptive Thresholds Based on Local Point Cloud Density. *ISPRS International Journal of Geo-Information* 10(3): 127. DOI: https://doi.org/10.3390/ijgi10030127.

Mahphood, A. and H. Arefi, 2017. A DATA DRIVEN METHOD FOR FLAT ROOF BUILDING RECONSTRUCTION FROM LiDAR POINT CLOUDS. *Int. Arch. Photogramm. Remote Sens. Spatial Inf. Sci.* 42: 167–172. DOI: https://doi.org/10.5194/isprs-archives-XLII-4-W4-167-2017.

Mahphood, A. and H. Arefi, 2020a. Tornado method for ground point filtering from LiDAR point clouds. *Advances in Space Research* 66(7): 1571-1592. DOI: https://doi.org/10.1016/j.asr.2020.06.030.

Mahphood, A. and H. Arefi, 2020b. Virtual first and last pulse method for building detection from dense LiDAR point clouds. *International Journal of Remote Sensing* 41(3): 1067-1092. DOI: https://doi.org/10.1080/01431161.2019.1655176.

Mahphood, A. and H. Arefi, 2022. Grid-based building outline extraction from ready-made building points. *Automation in Construction* 139: 104321. DOI: https://doi.org/10.1016/j.autcon.2022.104321.

Maltezos, E. and C. Ioannidis, 2015. AUTOMATIC DETECTION OF BUILDING POINTS FROM LIDAR AND DENSE IMAGE MATCHING POINT CLOUDS. *ISPRS Ann. Photogramm. Remote Sens. Spatial Inf. Sci.* DOI: 10.5194/isprsannals-II-3-W5-33-2015.

Mongus, D. and B. Žalik, 2012. Parameter-free ground filtering of LiDAR data for automatic DTM generation. *ISPRS Journal of Photogrammetry and Remote Sensing* 67: 1-12. DOI: https://doi.org/10.1016/j.isprsjprs.2011.10.002.

Neidhart, H. and M. Sester, 2008. Extraction of building ground plans from LiDAR data. *Int. Arch. Photogramm. Remote Sens. Spatial Inf. Sci.* 37(PART B2): 405-410.

Niemeyer, J., C. Mallet, F. Rottensteiner and U. Sörgel, 2011. Conditional random fields for the classification of LiDAR point clouds. *Int. Arch. Photogramm. Remote Sens. Spatial Inf. Sci.* 38(Part 4): W19.

Rutzinger, M., F. Rottensteiner and N. Pfeifer, 2009. A comparison of evaluation techniques for building extraction from airborne laser scanning. *IEEE Journal of selected topics in applied earth observations and remote sensing* 2(1): 11-20. DOI: https://doi.org/10.1109/JSTARS.2009.2012488.

Sajadian, M. and H. Arefi, 2014. a Data Driven Method for Building Reconstruction from LiDAR Point Clouds. *Int. Arch. Photogramm. Remote Sens. Spatial Inf. Sci.* 40(2): 225.

Shiravi, S., M. Zhong and S. A. Beykaei, 2012. Accuracy assessment of building extraction using LiDAR data for urban planning/transportation applications. *Conference of the Transportation Association of Canada*.

Tarsha-Kurdi, F., M. Rehor, T. Landes, P. Grussenmeyer and H. P. Baehr, 2007. Extension of an automatic building extraction technique to airborne laser scanner data containing damaged buildings. *ISPRS Hannover Workshop, Germany, High-Resolution Earth Imaging for Geospatial Information*, Germany. 1-6.

Tarsha Kurdi, F., M. Awrangjeb and N. Munir, 2021. Automatic filtering and 2D modeling of airborne laser scanning building point cloud. *Transactions in GIS* 25(1): 164-188. DOI: https://doi.org/10.1111/tgis.12685.

Vögtle, T. and E. Steinle, 2005. Fusion of 3D building models derived from first and last pulse laserscanning data. *Information Fusion* 6(4): 275-281. DOI: 10.1016/j.inffus.2004.06.010.

Widyaningrum, E., B. Gorte and R. Lindenbergh, 2019. Automatic building outline extraction from ALS point clouds by ordered points aided hough transform. *Remote Sensing* 11(14): 1727. DOI: https://doi.org/10.3390/rs11141727.

Yastikli, N. and Z. Cetin, 2021. Classification of raw LiDAR point cloud using point-based methods with spatial features for 3D building reconstruction. *Arabian Journal of Geosciences* 14(3): 1-14. DOI: https://doi.org/10.1007/s12517-020-06377-5.

Yi, Z., H. Wang, G. Duan and Z. Wang, 2021. An airborne LiDAR building-extraction method based on the naive Bayes–RANSAC method for proportional segmentation of quantitative features. *Journal of the Indian Society of Remote Sensing* 49(2): 393-404. DOI: https://doi.org/10.1007/s12524-020-01222-4.

Zeybek, M. and İ. Şanlıoğlu, 2019. Point cloud filtering on UAV based point cloud. *Measurement* 133: 99-111. DOI: https://doi.org/10.1016/j.measurement.2018.10.013.